

# Bose-Einstein Condensate in a Honeycomb Optical Lattice: Fingerprint of Superfluidity at the Dirac Point

Zhu Chen<sup>1</sup> and Biao Wu<sup>2</sup>

<sup>1</sup>*Institute of Physics, Chinese Academy of Sciences, 100190, Beijing, China*

<sup>2</sup>*International Center for Quantum Materials, Peking University, 100871, Beijing, China*

(Dated: March 7, 2019)

Mean-field Bloch bands of a Bose-Einstein condensate in a honeycomb optical lattice are computed. We find that the topological structure of the Bloch bands at the Dirac point is changed completely by the atomic interaction of arbitrary small strength: the Dirac point is extended into a closed curve and an intersecting tube structure arises around the original Dirac point. These tubed Bloch bands are caused by the superfluidity of the system. Furthermore, they imply the inadequacy of the tight-binding model to describe an interacting Boson system around the Dirac point and the breakdown of adiabaticity by interaction of arbitrary small strength.

PACS numbers: 67.85.Hj, 03.75.Kk, 37.10.Jk,

Inspired by the exciting physics in graphene[1–5], there have been increasing efforts to study ultracold atoms in a honeycomb optical lattice [6–12]. The primary reason is that this ultracold-atom system offers greater controlling flexibility over graphene[13, 14]. For example, with this hexagonal ultracold-atom system, one can readily change the lattice strength, tune the atomic scattering strength with Feshbach resonance, and load either bosons or fermions or even a mixture of bosons and fermions in the lattice. For example, there have already been efforts to study conical diffraction[7–9] and observe quantum phases with ultracold bosons in a honeycomb lattice[10]. This controlling flexibility will not only offer deeper insight into the graphene properties but also open up windows for physics beyond graphene.

In this Letter we provide an insight into the interplay between superfluidity and Dirac dynamics by studying a Bose-Einstein condensate (BEC) in a honeycomb optical lattice. To showcase the interplay, we compute the lowest Bloch bands for this BEC system. We find that the topology of the Bloch bands around the Dirac point is completely altered by an arbitrary small atomic interaction: an intersecting tube structure appears and the Dirac point is turned into a closed curve. We show that the topological change can be viewed a permanent fingerprint left in the Bloch bands by superfluidity. As the tight-binding model with on-site interaction does not change the Dirac point structure, this topological change suggests that tight-binding model is insufficient to describe the bosonic dynamics in a honeycomb lattice. At the same time, these tubed bands imply the breakdown of adiabaticity by arbitrary small atomic interaction. Feasible experimental schemes are suggested to observe this phenomenon.

The honeycomb optical lattice can be experimentally realized by three interfering traveling laser beams[15, 16], and is described mathematically by

$$V(\mathbf{r}) = V_0 \left[ \cos(\mathbf{b}_1 \cdot \mathbf{r}) + \cos(\mathbf{b}_2 \cdot \mathbf{r}) + \cos((\mathbf{b}_1 + \mathbf{b}_2) \cdot \mathbf{r}) \right], \quad (1)$$

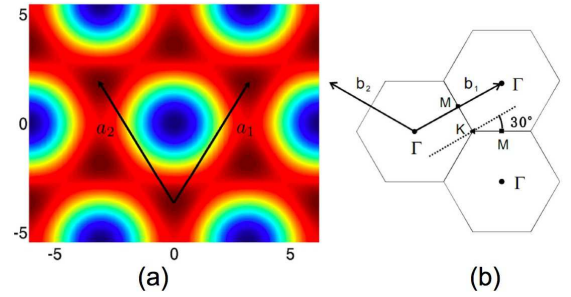


FIG. 1: (color online) (a) Contour map of the hexagonal potential in Eq.(2). The potential well is represented in red and the barrier in blue. The unit vectors are marked as  $\mathbf{a}_1$  and  $\mathbf{a}_2$ . (b) Unit cell in the reciprocal space with unit vectors  $\mathbf{b}_1$ ,  $\mathbf{b}_2$  and the high symmetry points  $\Gamma$ ,  $M$  and  $K$ .

where the reciprocal unit vectors  $\mathbf{b}_1 = 2\pi(\sqrt{3}, 1)/(\sqrt{3}a)$  and  $\mathbf{b}_2 = 2\pi(-\sqrt{3}, 1)/(\sqrt{3}a)$  with  $a = 2\lambda_L/3$ .  $\lambda_L$  is the wavelength of the laser beams. We are interested in the superfluid regime, where the system can be well described by the Gross-Pitaevskii (GP) equation

$$i\hbar \frac{\partial \psi}{\partial t} = -\frac{\hbar^2}{2m} \nabla^2 \psi + V(\mathbf{r})\psi + \frac{4\pi\hbar^2 a_s}{m} |\psi|^2 \psi. \quad (2)$$

with  $m$  the mass of particle and  $a_s$  the scattering length. For numerical computation, the above equation is made dimensionless by normalizing the wave function and choosing  $6E_R$  as energy unit with  $E_R = \hbar^2 k_L^2/2m$ ,  $ma^2/3\pi^2\hbar$  as the time unit, and  $2\pi a$  as the length unit. The scaled nonlinearity and potential strength are denoted as  $c$  and  $v$  respectively.

We focus on the Bloch wave solutions of the GP equation, which are of the form  $\psi_{\mathbf{k}}(\mathbf{r}) = \sum_{m,n} c_{mn} e^{i(\mathbf{k} + \mathbf{G}_{mn}) \cdot \mathbf{r}}$  with  $\mathbf{G}_{mn} = m\mathbf{b}_1 + n\mathbf{b}_2$ . We have computed numerically the nonlinear Bloch bands for the hexagonal BEC system. The results are shown in Fig.2. Compared to the linear bands in Fig.2(a), we see that the nonlinear bands in (b) have a similar overall structure. However, the part

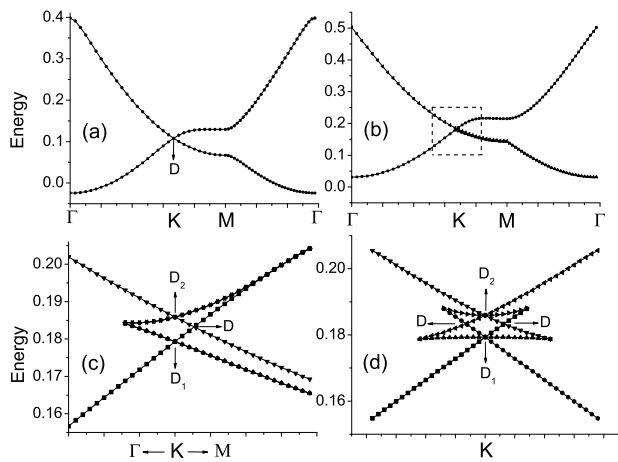


FIG. 2: Bloch bands along the high symmetry points. (a) The linear case.  $c = 0$ ,  $v = 0.1$ .  $D$  marks the Dirac point at point  $\mathbf{K}$ . (b) The nonlinear case.  $c = 0.1$ ,  $v = 0.1$ . (c) The enlarged rectangle part in (b). There appear two additional crossing points  $D_1$  and  $D_2$  while the linear Dirac point  $D$  is shifted away from  $\mathbf{K}$ . (d) The band structure along the direction represented by the dashed line in Fig.1(b).

around point  $\mathbf{K}$  appears to be modified by nonlinearity. When it is enlarged, we find in (c) that the two linear bands have split into four bands. As a result, two more additional crossing points  $D_1$  and  $D_2$  appear while the Dirac crossing  $D$  is shifted away from point  $\mathbf{K}$ . This feature is also clear in (d), where the Bloch band along the direction  $30^\circ$  off the  $\mathbf{K}$ - $\mathbf{M}$  axis is plotted. We have also plotted the nonlinear Bloch band near point  $\mathbf{M}$  in Fig.4(b) where we see a loop structure, very similar to the BEC Bloch bands in one dimensional optical lattice. We further notice that when the nonlinearity  $c$  is small enough, the loop structure at  $\mathbf{M}$  will disappear. In stark contrast, the nonlinear structure around  $\mathbf{K}$  as seen in Fig.2(c) exists for arbitrary small value of  $c$ . We will fully examine this feature in later discussion.

The full BEC Bloch bands near point  $\mathbf{K}$  are plotted in Fig.3(d). The complicated Bloch bands consist of three “tubes”, which intersect at point  $\mathbf{K}$  and are sandwiched by two Dirac cones. One of the tubes is shown in Fig.3(a): it lies along the  $\mathbf{M}$ - $\mathbf{K}$  direction and it has a wedged cross-section. Fig.3(b) shows the cross-section of two intersecting tubes. The two green dots mark the top and bottom tips of this intersection and correspond to  $D_1$  and  $D_2$  points in Fig.2(c,d). The red dots indicate part of a closed curve, which results from the intersection of the three tubes; the shifted Dirac point  $D$  in Fig. 2(c,d) is one of the points on this closed curve. This shows that the Dirac point is turned into a closed curve by the interaction. The size of the three intersecting tubes becomes smaller as the interaction strength  $c$  gets weaker. However, surprisingly, the tubes disappear only when  $c$  is zero. Note that the tips of the Dirac cones in

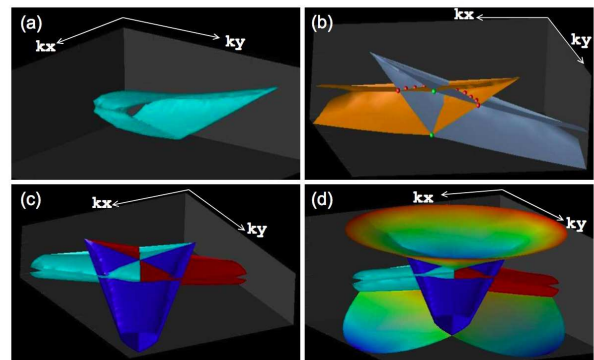


FIG. 3: (color) The lowest nonlinear Bloch bands around point  $\mathbf{K}$ . (a) One of three “tubes”; (b) the cross-section of two intersecting “tubes”; (c) the crossing of the three “tubes”; (d) the full bands. The green dots are  $D_1$  and  $D_2$  points in Fig.2(c) while the red dots indicate a closed loop where the  $D$  point in Fig.2(c) belongs.  $v = 0.1$ ,  $c = 0.1$ .

Fig.3(d) have only triangular symmetry, and do not have the cylindrical symmetry as in the linear case.

We emphasize that the appearance of the tube structure in the BEC Bloch bands for arbitrary small  $c$  is a unique feature in a honeycomb lattice. In one dimensional lattice[17–22] and two dimensional square lattice[23, 24], the loop or tube nonlinear structure in the BEC Bloch bands appears only when  $c$  is bigger than a critical value. One intuitive way to understand this is as follows. At the Dirac point, the Bloch wave function has a triangular symmetry. As a result, the effective potential  $V(\mathbf{r}) + c|\psi(\mathbf{r})|^2$  in Eq.(2) loses the hexagonal symmetry of the honeycomb lattice as long as  $c$  is not zero, and therefore destroys the delicate Dirac point at  $\mathbf{K}$ .

This tubed structure can be viewed as a fingerprint left in the Bloch bands by the superfluidity of the BEC systems. Assume that we have a mass flow of boson particles, which is represented by plane wave  $e^{ikx}$  with  $k$  at the Brillouin zone (BZ) edge point  $\mathbf{M}$ . We now slowly turn on an optical lattice of small lattice strength. For free bosons, the flow is stopped by the Bragg scattering, the plane wave assumes the form of  $\sin(kx)$ . In the energy band, this is reflected by that the crossing of two plane wave energy bands at  $\mathbf{M}$  is replaced by a gap as seen in Fig.4(a). In the nonlinear case, the situation can be very different: when the interaction is strong so that the superfluid critical velocity is larger than  $k$ , the small optical lattice, which can be regarded as perturbation, should not stop the super-flow. This implies that the wave function describing the flow should still resemble the plane wave  $e^{ikx}$ , and at the same time, the crossing of plane wave energy bands should remain unchanged. This is confirmed by our numerical calculation shown in Fig.4(b). When this superfluidity argument is applied to other points along the BZ edge, we should have a tubed structure seen in Fig.3. In other words, we can view the

tubed structure as the fingerprint left in the BEC Bloch bands by superfluidity. For this hexagonal system, this fingerprint stays as long as  $c$  is not zero.

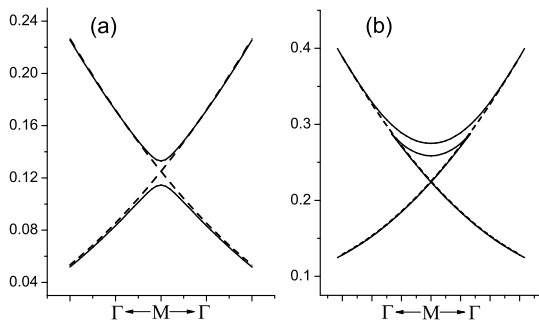


FIG. 4: The lowest Bloch bands for a honeycomb lattice at the  $\Gamma$ -M- $\Gamma$  branch. (a) Free boson; (b) BEC. The solid curves are Bloch bands while the dashed curves are the energy of the plane waves.

As is well known, when the lattice is deep, it is believed that the system can be well described by a tight-binding model. However, as shown below, the tight-binding model is not an adequate approximation for a BEC in a honeycomb lattice no matter how deep the lattice is. Following the usual procedure[11], we break up the bosonic field into a sum over the two sublattices  $\psi = \sum_{\vec{a}} \psi_{\vec{a}} u(\vec{r} - \vec{a}) + \sum_{\vec{b}} \psi_{\vec{b}} u(\vec{r} - \vec{b})$ , where  $u(\vec{r})$  is the Wannier function and  $\vec{a}$  and  $\vec{b}$  are lattice vectors in the two sub-lattices, respectively. Then the tight-binding Hamiltonian for our BEC system is

$$H = -J \sum_{\langle \vec{a}, \vec{b} \rangle} (\psi_{\vec{a}}^* \psi_{\vec{b}} + \text{h.c.}) + \frac{U}{2} \left[ \sum_{\vec{a}} |\psi_{\vec{a}}|^4 + \sum_{\vec{b}} |\psi_{\vec{b}}|^4 \right], \quad (3)$$

where  $J$  is the hopping constant and  $U$  is the on-site interaction proportional to  $c$ . The ground state energy is  $E = -J|\Sigma| + \frac{1}{2}U$ , where  $\Sigma = \sum_{\vec{\delta}} e^{i\mathbf{k} \cdot \vec{\delta}}$  with the summation over all the three vectors  $\vec{\delta}$  connecting nearest neighbors. For a wave vector deviate slightly from point  $\mathbf{K}$ , we have  $E \sim \frac{\sqrt{3}}{2}Jq + U/2$ , where  $q$  is the small de-

viation. This recovers the massless Dirac cone structure. In other words, the tight-binding model can not produce the tube-intersecting structure seen in Fig.3. Combined with the aforementioned fact that the tube structure in Fig.3 appears for arbitrary small interaction strength  $c$ , this implies that the tight-binding model is not an adequate approximation for a BEC in a honeycomb lattice no matter how deep the lattice is. This is a very surprising result compared to the situation in one dimensional lattice[17, 18] and in two dimensional square lattice[23, 24]. In these two cases, the loop or tube structure will disappear when  $c$  is smaller than a finite value or the lattice is deep enough. This means that the tight-binding model is a good approximation in these two cases when the lattice is deep enough.

We have also checked the stabilities of the BEC Bloch waves around the Dirac point. We find that most of these Bloch waves are dynamically unstable with the GP equation, similar to we found in the square lattice[25]. However, our analysis with the tight-binding model shows that all the BEC Bloch waves around the Dirac point are stable. This is another contradiction between the tight-binding model and the continuous GP equation, further indicating that the tight-binding model is not a proper model for a BEC in a honeycomb lattice. It would be very interesting in the future to check how well the quantum version of the tight-binding model, the Bose-Hubbard model, can describe bosons in a honeycomb lattice.

Let us look further into the physical meaning of the tube structure shown in Fig.3. As been explored before, the loop structure in the one dimensional optical lattice implies the breakdown of adiabaticity by strong enough nonlinearity. This interesting effect has not only been generalized to general nonlinear quantum systems[26] but also been observed experimentally with ultra-cold atoms[27]. Similarly, this tube structure in Fig.3 also implies the breakdown of adiabaticity. In fact, it goes beyond. As we have pointed out several times, the tube structure appears for arbitrary small nonlinearity. This means that the adiabaticity can be broken down by arbitrary small interaction in this hexagonal BEC system. This interesting phenomenon can be illustrated more clearly when we approximate this BEC system at point  $\mathbf{K}$  with a three-mode model. The three-mode model is

$$i \frac{\partial}{\partial t} \begin{pmatrix} \phi_1 \\ \phi_2 \\ \phi_3 \end{pmatrix} = \begin{pmatrix} -|\phi_1|^2 c - \frac{\delta k_x}{4} - \frac{\sqrt{3}\delta k_y}{2} & v/2 & v/2 \\ v/2 & -|\phi_2|^2 c + \frac{\delta k_x}{2} & v/2 \\ v/2 & v/2 & -|\phi_3|^2 c - \frac{\delta k_x}{4} + \frac{\sqrt{3}\delta k_y}{2} \end{pmatrix} \begin{pmatrix} \phi_1 \\ \phi_2 \\ \phi_3 \end{pmatrix}, \quad (4)$$

where  $\delta k_x$  and  $\delta k_y$  denote how much the Bloch wave

number  $\mathbf{k}$  deviates away from  $\mathbf{K}$ .

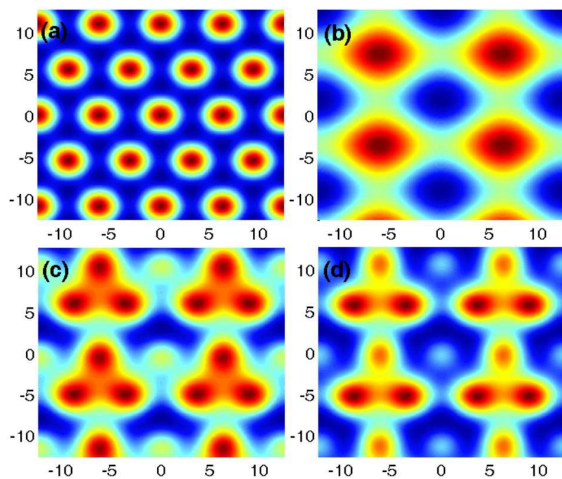


FIG. 5: (color online) (a) The triangular optical lattice  $V_{\text{tri}}$ ; (b) the rectangular optical lattice  $V_{\text{rec}}(\theta)$ . Superposition of these two lattices with (c)  $\theta = -7\pi/12$  and (d)  $\theta = -\pi/4$ . The potential well is represented in red and the barrier in blue.

This three-mode model can also describe a BEC in a triple-well potential, where the three wells are arranged in a triangular geometry with the depth of each well adjustable[28, 29]. It should also be realized in experiment with waveguide systems[30–32]. This shows that this breakdown of adiabaticity by arbitrary small interaction is general and can happen in a wide range of systems.

Inspired by the experiment in [27], we here propose a scheme to realize the above mentioned triple well configuration. The explicit procedure is illustrated in Fig.5. At first, a triangular lattice is formed by three lasers as shown in Fig.5(a). The potential can be described by  $V_{\text{tri}} = V_0 \left[ \cos(x + \frac{y}{\sqrt{3}}) + \cos(-x + \frac{y}{\sqrt{3}}) + \cos(\frac{2y}{\sqrt{3}}) \right]$  with  $V_0 < 0$ . The second step is to form the triple-well systems by adding a rectangular lattice  $V_{\text{rec}}(\theta) = V_1 \left[ \cos(x/2) + \cos((y + \theta)/\sqrt{3}) \right]$  ( $V_1 > 0$ ). As changing  $\theta$ , as shown in Fig. 5(c,d), the second optical lattice can not only break the triangular lattice into a series of independent triple-well systems and but also change the depth of each well. One should be able to demonstrate the breakdown of adiabaticity by arbitrary small interaction with this triple-well system, similar to the experiment done in Ref. [27].

We have computed the BEC Bloch bands in a honeycomb optical lattice. Our results show that a tube-intersecting structure can emerge between the up and down Dirac cones for arbitrary small interaction. This structure has two interesting physical implications: (1) the tight-bind model can not describe adequately the BEC in a honeycomb lattice even when the lattice is very deep; (2) the adiabaticity can be broken down by arbitrary small interaction in certain systems. For the latter, we have proposed an experimental scheme to observe it.

We thank Yongping Zhang for useful discussions. We also thank Zhaoxing Liang for the help on numerical calculation. This work was supported by the NSF of China (10825417).

- 
- [1] K. S. Novoselov *et al.*, *Nature* **438**, 197 (2005).
  - [2] A. K. Geim and K. S. Novoselov, *Nature Materials* **6**, 183 (2007).
  - [3] C. Wu, D. Bergman, L. Balents, and S. DasSarma, *Phys. Rev. Lett.* **99**, 070401 (2007).
  - [4] G. Li and E. Y. Andrei, *Nat. Phys.* **3**, 623 (2007).
  - [5] A. H. C. Neto, F. Guinea, N. M. R. Peres, K. S. Novoselov, and A. K. Geim, *Rev. Mod. Phys.* **81**, 109 (2009).
  - [6] S.-L. Zhu, B. Wang, and L.-M. Duan, *Phys. Rev. Lett.* **98**, 260402 (2007).
  - [7] M. J. Ablowitz, S. D. Nixon, and Y. Zhu, *Phys. Rev. A* **79**, 053830 (2009).
  - [8] O. Bahat-Treidel, O. Peleg, M. Segev, and H. Buljan, *Phys. Rev. A* **82**, 013830 (2010).
  - [9] O. Peleg, G. Bartal, B. Freedman, O. Manela, M. Segev, and D. N. Christodoulides, *Phys. Rev. Lett.* **98**, 103901 (2007).
  - [10] Parvis Soltan-Panahi *et al.*, arXiv:1005.1276 (2010).
  - [11] L. H. Haddad and L. D. Carr, cond-mat/1006.3893.
  - [12] L. H. Haddad and L. D. Carr, *Physica D: Nonlinear Phenomena* **238**, 1413 (2009).
  - [13] O. Morsch and M. Oberthaler, *Rev. Mod. Phys.* **78**, 179 (2006).
  - [14] V. Yukalov, *Laser Physics* **19**, 1 (2009).
  - [15] G. Grynberg, B. Lounis, P. Verkerk, J. Y. Courtois, and C. Salomon, *Phys. Rev. Lett.* **70**, 2249 (1993).
  - [16] B. Wunsch, F. Guinea, and F. Sols, *New J. Phys.* **10**, 103027 (2008).
  - [17] B. Wu and Q. Niu, *New J. Phys.* **5**, 104 (2003).
  - [18] B. Wu and Q. Niu, *Phys. Rev. A* **61**, 023402 (2000).
  - [19] M. Machholm, C. J. Pethick, and H. Smith, *Phys. Rev. A* **67**, 053613 (2003).
  - [20] B. T. Seaman, L. D. Carr, and M. J. Holland, *Phys. Rev. A* **72**, 033602 (2005).
  - [21] B. T. Seaman, L. D. Carr, and M. J. Holland, *Phys. Rev. A* **72**, 033602 (2005).
  - [22] E. J. Mueller, *Phys. Rev. A* **66**, 063603 (2002).
  - [23] Z. Chen, Z. Liang, and B. Wu, unpublished.
  - [24] C.-S. Chien, S.-L. Chang, and B. Wu, *Comput. Phys. Commun.* **181**, 1727 (2010).
  - [25] Z. Chen and B. Wu, *Phys. Rev. A* **81**, 043611 (2010).
  - [26] J. Liu, B. Wu, and Q. Niu, *Phys. Rev. Lett.* **90**, 170404 (2003).
  - [27] Y.-A. Chen, S. D. Huber, S. Trotzky, I. Bloch, and E. Altman, *Nature Phys.* **7**, 61 (2010).
  - [28] R. Franzosi and V. Penna, *Phys. Rev. E* **67**, 046227 (2003).
  - [29] X. Jiang, L.-B. Fu, W. shan Duan, and J. Liu, *J. Phys. B: At., Mol. Opt. Phys.* **181**, 1727 (2010).
  - [30] X. Luo, Q. Xie, and B. Wu, *Phys. Rev. A* **76**, 051802(R) (2007).
  - [31] A. Szameit *et al.*, *Opt. Lett.* **34**, 2700 (2009).
  - [32] A. S. Desyatnikov *et al.*, *Opt. Lett.* **32**, 325 (2007).